Frontiers of Physics
https://doi.org/10.1007/s11467-021-1098-1
Front. Phys.
16(6), 61501 (2021)

RESEARCH ARTICLE

Transferring quantum entangled states between multiple single-photon-state qubits and coherent-state qubits in circuit QED

Qi-Ping Su[1], Hanyu Zhang[1], Chui-Ping Yang[1,2,†]

[1] *Department of Physics, Hangzhou Normal University, Hangzhou 311121, China*
[2] *Quantum Information Research Center, Shangrao Normal University, Shangrao 334001, China*
Corresponding author. E-mail: [†] *yangcp@hznu.edu.cn*
Received September 24, 2020; accepted June 23, 2021

We present a way to transfer maximally- or partially-entangled states of n single-photon-state (SPS) qubits onto n coherent-state (CS) qubits, by employing $2n$ microwave cavities coupled to a superconducting flux qutrit. The two logic states of a SPS qubit here are represented by the vacuum state and the single-photon state of a cavity, while the two logic states of a CS qubit are encoded with two coherent states of a cavity. Because of using only one superconducting qutrit as the coupler, the circuit architecture is significantly simplified. The operation time for the state transfer does not increase with the increasing of the number of qubits. When the dissipation of the system is negligible, the quantum state can be transferred in a deterministic way since no measurement is required. Furthermore, the higher-energy intermediate level of the coupler qutrit is not excited during the entire operation and thus decoherence from the qutrit is greatly suppressed. As a specific example, we numerically demonstrate that the high-fidelity transfer of a Bell state of two SPS qubits onto two CS qubits is achievable within the present-day circuit QED technology. Finally, it is worthy to note that when the dissipation is negligible, entangled states of n CS qubits can be transferred back onto n SPS qubits by performing reverse operations. This proposal is quite general and can be extended to accomplish the same task, by employing a natural or artificial atom to couple $2n$ microwave or optical cavities.

Keywords entangled state, single-photon-state qubit, coherent-state qubit, circuit QED

1 Introduction

Discrete- and continuous-variable methods to optical quantum communication and quantum information processing (QIP) rely on different encoding qubits for their realization [1–3]. For the discrete-variable approaches, single photons are involved [4, 5], the photonic qubits live in a two-dimensional Hilbert space formed, for instance, by orthogonal polarizations or the absence and presence of a single photon. For convenience, we define such photonic qubits as single-photon-state (SPS) qubits. In contrast, for the continuous-variable approaches, encoding is implemented in the quadrature components of a light field with an inherently infinite-dimensional space. Quantum information carried by a qubit can be indicated as an arbitrary superposition of coherent states or an arbitrary superposition of cat states of light waves [6, 7]. In recent years, besides progress achieved with SPS qubits, considerable theoretical and experimental activity have also been shifted to QIP with coherent-state (CS) or cat-state (C-S) qubits. There exists a number of works for QIP using qubits encoded with coherent states [6, 8–10] or encoded with cat-state qubits [7, 11–16].

Both encodings of SPS qubits and CS/C-S qubits have advantages and drawbacks [17]. CS/C-S qubits benefit from unconditional operations, unambiguous state discrimination, high detection efficiencies, and more practical interfacing with conventional information technology. However, it is commonly recognized that quantum states of multiphoton wave fields are difficult to manipulate and suffer from intrinsically limited fidelities. On the other hand, quantum states of SPS qubits are relatively easy to operate, but usually suffer from decoherence due to the loss of a single photon. A combination of qubits with different encodings, that is, in a hybrid architecture [18], may offer great advantages [19]. Some operations may be more efficient using SPS qubits while others may better take advantage of CS/C-S qubits. In this endeavour, it is a key requirement to transfer information or entanglement between qubits with different encodings.

The goal of this work is aimed at transferring the fol-

* This article can also be found at http://journal.hep.com.cn/fop/EN/10.1007/s11467-021-1098-1.

lowing type of entangled state

$$c\left|i_1\right\rangle\left|i_2\right\rangle\cdots\left|i_n\right\rangle+d\left|\bar{i}_1\right\rangle\left|\bar{i}_2\right\rangle\cdots\left|\bar{i}_n\right\rangle \tag{1}$$

between n SPS qubits and n CS qubits. For $c\neq d$, the state (1) is a *partially-entangled* state. For $c=d=1/\sqrt{2}$, the state (1) is a *maximally-entangled* state, which is called Bell state when $n=2$ or Greenberger–Horne–Zeilinger (GHZ) state when $n\geq 3$. As is well known, Bell states and GHZ states are crucial resources and play an important role in quantum communication and QIP. On the other hand, transferring entangled states between qubits of different encodings is of fundamental interest in quantum mechanics, and may be necessary and important in the hybrid quantum communication and QIP. For instance, in a hybrid QIP based on SPS qubits and CS qubits, entanglement transfer may be necessary between SPS-qubit-based quantum processors and CS-qubit-based quantum processors.

The new and rapidly growing field of circuit QED, consisting of microwave radiation fields and fixed artificial atoms, offers extremely exciting prospects for solid-state QIP [20–28]. In the following, we will present an approach to transfer the entangled state (1) between n SPS qubits and n CS qubits, in a circuit QED system that consists of $2n$ microwave cavities coupled to a superconducting flux qutrit. In our proposal, the two logic states $|i\rangle$ and $|\bar{i}\rangle$ of a SPS qubit are denoted as the vacuum state $|0\rangle$ and the single-photon state $|1\rangle$ of a cavity; while the two logic states $|i\rangle$ and $|\bar{i}\rangle$ of a CS qubit are indicated by the two coherent states $|\pm\alpha\rangle$ of a cavity, which can be quasi-orthogonal for a sufficiently large α (for instance, $|\langle\alpha|-\alpha\rangle|=\mathrm{e}^{-2|\alpha|^2}\sim 10^{-3}$ for $\alpha=1.86$). As is well known, coherent states are eigenstates of the photon annihilation operator and thus tolerant to single-photon loss [11].

In this work, we will explicitly show how to transfer the entangled state (1) from n SPS qubits onto n CS qubits. Note that since no measurement is involved, i.e., all basic operations are unitary, the entangled state (1) can be transferred back from n CS qubits onto n SPS qubits by performing reverse operations, in the case when the dissipation of the system is negligible.

The present proposal has the following features: (i) Because only one superconducting flux qutrit is used, the circuit complexity is reduced; (ii) The state transfer time is independent of the number of qubits, thus it does not increase with the increase of the number of qubits; (iii) The higher-energy level of the qutrit is not excited during the entire operation, thus the effect of decoherence from this level is suppressed; and (iv) Since measurement is not required, the entangled state can be transferred in a deterministic manner when the dissipation is negligible. This proposal is universal and can be applied to accomplish the same task, in a physical system which consists of $2n$ microwave or optical cavities coupled to a natural or artificial atom. To the best of our knowledge, how to transfer quantum entangled states between SPS qubits and CS qubits has not been reported yet.

We should point out that this proposal works by applying the rotating-wave approximation (RWA). As is well known, the RWA is often used in quantum optics and quantum information processing. As an open question, it would be interesting to generalize the protocol to a more general case without assuming the RWA, which usually applies in the ultrastrong coupling regime (for a review, see [29]).

This paper is organized as follows. In Section 2, we introduce a few types of interaction and state evolution, which are used for transferring entangled states. In Section 3, we show how to transfer the entangled states of n SPS qubits onto n CS qubits. In Section 4, as an example, we investigate the experimental feasibility for transferring a Bell state of two SPS qubits onto two CS qubits in a circuit QED setup. A brief conclusion is given in Section 5.

2 Type of interaction and state evolution

Consider n single-mode cavities $(1,2,\cdots,n)$ and another n single-mode cavities $(1',2',\cdots,n')$. The $2n$ cavities are connected by a superconducting flux qutrit A (Fig. 1(a). The three levels of the coupler qutrit are labelled as $|g\rangle$, $|e\rangle$,and $|f\rangle$ [Fig. 1(b)]. In this section, we will introduce a few types of interaction, the corresponditing

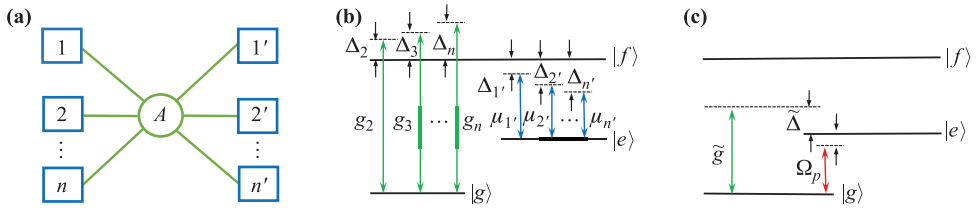

Fig. 1 **(a)** Diagram of $2n$ microwave cavities coupled to a superconducting flux qutrit (the circle A in the middle). Each square represents a cavity, which can be a one- or three-dimensional cavity. The qutrit is capacitively or inductively coupled to each cavity. **(b)** Illustration of $n-1$ cavities $(2,3,\cdots,n)$ off resonant with the $|g\rangle\leftrightarrow|f\rangle$ transition of the qutrit, while n cavities $(1',2',\cdots,n')$ off resonant with the $|e\rangle\leftrightarrow|f\rangle$ transition of the qutrit. **(c)** Illustration of cavity $1'$ and a microwave pulse off resonant with the $|g\rangle\leftrightarrow|e\rangle$ transition of the qutrit.

Hamiltonians, and the state evolutions, which will be used for the entangled state transfer in next section.

2.1 Qutrit-cavity resonant interaction

Consider cavity 1 on resonance with the $|g\rangle \leftrightarrow |e\rangle$ transition of the qutrit. In the interaction picture and after making the rotating-wave approximation (RWA), the Hamiltonian is given by (hereafter assuming $\hbar = 1$)

$$H_1 = g_r \hat{a}_1 \sigma_{eg}^{+} + \text{h.c.}, \tag{2}$$

where $\sigma_{eg}^{+} = |e\rangle\langle g|$, g_r is the coupling strength between cavity 1 and the $|g\rangle \leftrightarrow |e\rangle$ transition, and $\hat{a}_1$ is the photon annihilation operator of cavity 1. Under this Hamiltonian, it is easy to get the following state evolution

$$\begin{aligned} &|e\rangle|0\rangle_1 \to \cos g_r t\,|e\rangle|0\rangle_1 - \mathrm{i}\sin g_r t\,|g\rangle|1\rangle_1, \\ &|g\rangle|1\rangle_1 \to \cos g_r t\,|g\rangle|1\rangle_1 - z\mathrm{i}\sin g_r t\,|e\rangle|0\rangle_1, \end{aligned} \tag{3}$$

while the state $|g\rangle|0\rangle_1$ remains unchanged.

2.2 Off-resonant interaction between the coupler qutrit and the $(2n-1)$ cavities

Consider that the qutrit is decoupled from cavity 1 but interacts with the $(2n-1)$ cavities $(2, 3, \cdots, n, 1', 2', \cdots, n')$. Assume that cavity j is off resonant with the $|g\rangle \leftrightarrow |f\rangle$ transition with coupling constant g_j and detuning Δ_j $(j = 2, 3, \cdots, n)$, while highly detuned (decoupled) from other intra-level transitions [Fig. 1(b)]. In addition, suppose that cavity j' is off resonant with the $|e\rangle \leftrightarrow |f\rangle$ transition with coupling constant $\mu_{j'}$ and detuning $\Delta_{j'}$ $(j' = 1', 2', \cdots, n')$, while highly detuned (decoupled) from other intra-level transitions [Fig. 1(b)]. After these considerations, in the interaction picture and after the RWA, the Hamiltonian is given by

$$\begin{aligned} H_2 = &\sum_{j=2}^{n} g_j \left(\mathrm{e}^{\mathrm{i}\Delta_j t}\hat{a}_j \sigma_{fg}^{+} + \text{h.c.}\right) \\ &+ \sum_{j'=1'}^{n'} \mu_{j'} \left(\mathrm{e}^{\mathrm{i}\Delta_{j'} t}\hat{b}_{j'} \sigma_{fe}^{+} + \text{h.c.}\right), \end{aligned} \tag{4}$$

where $\hat{a}_j$ $(\hat{b}_{j'})$ is the photon annihilation operator of cavity j (j'); $\sigma_{fg}^{+} = |f\rangle\langle g|$, $\sigma_{fe}^{+} = |f\rangle\langle e|$, $\Delta_j = \omega_{fg} - \omega_{c_j}$ and $\Delta_{j'} = \omega_{fe} - \omega_{c_{j'}}$. Here, ω_{fg} (ω_{fe}) is the $|g\rangle \leftrightarrow |f\rangle$ $(|e\rangle \leftrightarrow |f\rangle)$ transition frequency of the qutrit, while ω_{c_j} $(\omega_{c_{j'}})$ is the frequency of cavity j (cavity j').

Under the large detunings $|\Delta_j| \gg g_j$ and $|\Delta_{j'}| \gg \mu_{j'}$, no energy exchange is induced between the coupler qutrit and the cavities. When the following conditions satisfy, i.e.,

$$\frac{|\Delta_j - \Delta_k|}{\left|\Delta_j^{-1}\right| + \left|\Delta_k^{-1}\right|} \gg g_j g_k, \frac{|\Delta_{j'} - \Delta_{k'}|}{\left|\Delta_{j'}^{-1}\right| + \left|\Delta_{k'}^{-1}\right|} \gg \mu_{j'}\mu_{k'},$$

$$\frac{|\Delta_j - \Delta_{k'}|}{\left|\Delta_j^{-1}\right| + \left|\Delta_{k'}^{-1}\right|} \gg g_j \mu_{k'}, \tag{5}$$

(where $j, k \in \{2,3,\cdots,n\}$, $j', k' \in \{1', 2', \cdots, n'\}$, $j \neq k$, $j' \neq k'$) no interaction between cavities $(2, 3, \cdots, n, 1', 2', \cdots, n')$ is induced by the coupler qutrit. Thus, from the Hamiltonian (4), one can obtain the following effective Hamiltonian [30, 31]

$$\begin{aligned} H_{\mathrm{e}} = &-\sum_{j=2}^{n} \frac{g_j^2}{\Delta_j}\left(\sigma_g \hat{a}_j^{+}\hat{a}_j - \sigma_f \hat{a}_j \hat{a}_j^{+}\right) \\ &-\sum_{j'=1'}^{n'} \frac{\mu_{j'}^2}{\Delta_{j'}}\left(\sigma_e \hat{b}_{j'}^{+}\hat{b}_{j'} - \sigma_f \hat{b}_{j'}\hat{b}_{j'}^{+}\right), \end{aligned} \tag{6}$$

where $\sigma_g = |g\rangle\langle g|, \sigma_e = |e\rangle\langle e|, \sigma_f = |f\rangle\langle f|$. In Eq. (6), the terms in the first line represent the ac-Stark shifts of the levels $|g\rangle$ and $|f\rangle$ induced by the cavities $(2, 3, \cdots, n)$, while the terms in the second line are the ac-Stark shifts of the levels $|e\rangle$ and $|f\rangle$ caused by the cavities $(1', 2', \cdots, n')$.

In the case of the level $|f\rangle$ being not occupied, the Hamiltonian (6) reduces to

$$H_{\mathrm{e}} = -\sum_{j=2}^{n} \lambda_j \sigma_g \hat{a}_j^{+}\hat{a}_j - \sum_{j'=1'}^{n'} \lambda_{j'} \sigma_e \hat{b}_{j'}^{+}\hat{b}_{j'}, \tag{7}$$

where $\lambda_j = g_j^2/\Delta_j$ and $\lambda_{j'} = \mu_{j'}^2/\Delta_{j'}$. Under this Hamiltonian (7), it is straightforward to obtain

$$\begin{aligned} &|g\rangle|0\rangle_j \to |g\rangle|0\rangle_j, \quad |g\rangle|1\rangle_j \to \mathrm{e}^{\mathrm{i}\lambda_j t}|g\rangle|1\rangle_j, \\ &|g\rangle|\alpha\rangle_{j'} \to |g\rangle|\alpha\rangle_{j'}, \\ &|e\rangle|0\rangle_j \to |e\rangle|0\rangle_j, \quad |e\rangle|1\rangle_j \to |e\rangle|1\rangle_j, \\ &|e\rangle|\alpha\rangle_{j'} \to |e\rangle\left|\mathrm{e}^{\mathrm{i}\lambda_{j'} t}\alpha\right\rangle_{j'}, \end{aligned} \tag{8}$$

where $j \in \{2, 3, \cdots, n\}$ and $j' \in \{1', 2', \cdots, n'\}$.

2.3 Driving the qutrit conditional on the cavity's state

Consider cavity $1'$ to be off resonant with the $|g\rangle \leftrightarrow |e\rangle$ transition of the qutrit, with coupling strength $\widetilde{g}$ and detuning $\widetilde{\Delta} = \omega_{eg} - \widetilde{\omega}_{c_{1'}}$ [Fig. 1(c)]. Here, $\widetilde{\omega}_{c_{1'}}$ is the adjusted frequency of cavity $1'$. Meanwhile, assume that a classical pulse of frequency ω_p and initial phase ϕ is applied to the qutrit.

Under the above assumptions, the Hamiltonian of the system in the interaction picture and after the RWA is given by

$$H_3 = \widetilde{g}\mathrm{e}^{\mathrm{i}\widetilde{\Delta}t}\hat{a}_{1'}\sigma_{eg}^{+} + \Omega_p \mathrm{e}^{-\mathrm{i}[(\omega_p - \omega_{eg})t + \phi]}\sigma_{eg}^{+} + \text{h.c.}, \tag{9}$$

where Ω_p is the Rabi frequency of the pulse.

Under the large detuning condition $\left|\widetilde{\Delta}\right| \gg \tilde{g}$, and assuming $\left|\widetilde{\Delta}\right| \gg \Omega_p$, we can obtain the following effective Hamiltonian [22, 31]

$$H_{\mathrm{e}} = \frac{\widetilde{g}^2}{\widetilde{\Delta}}\left(\hat{a}_{1'}^{+}\hat{a}_{1'} + \frac{1}{2}\right)\sigma_z$$

$$+\left(\Omega_p e^{-i[(\omega_p-\omega_{eg})t+\phi]}\sigma_{eg}^{+}+\text{h.c.}\right), \tag{10}$$

where $\sigma_z = |e\rangle\langle e| - |g\rangle\langle g|$. Here, the stark-shift effect of the qubit induced by the pulse is negligible because of $\left|\widetilde{\Delta}\right| \gg \Omega_p$. In a rotating frame under the Hamiltonian $H_0 = \frac{\widetilde{g}^2}{\widetilde{\Delta}}\left(\hat{a}_{1'}^{+}\hat{a}_{1'} + \frac{1}{2}\right)\sigma_z$, and for $\omega_p = \omega_{eg} + \widetilde{g}^2/\widetilde{\Delta}$, one obtains

$$H_e = \Omega_p e^{-i\phi} e^{i4\widetilde{\omega}\hat{a}_{1'}^{+}\hat{a}_{1'}t}\sigma_{eg}^{+} + \text{h.c.}, \tag{11}$$

where $\widetilde{\omega} = \widetilde{g}^2/\left(2\widetilde{\Delta}\right)$. When the cavity is in the vacuum state, one can easily find that this Hamiltonian reduce to $H_{\text{eff}} = \Omega_p e^{-i\phi}\sigma_{eg}^{+} + \text{H.c.}$, which rotates the qubit's state as follows

$$\begin{aligned} |g\rangle|0\rangle_{1'} &\to \left(\cos\Omega_p t\,|g\rangle - ie^{-i\phi}\sin\Omega_p t\,|e\rangle\right)|0\rangle_{1'}, \\ |e\rangle|0\rangle_{1'} &\to \left(-ie^{i\phi}\sin\Omega_p t\,|g\rangle + \cos\Omega_p t\,|e\rangle\right)|0\rangle_{1'}. \end{aligned} \tag{12}$$

On the other hand, when the cavity is in the coherent state $|2\alpha\rangle$, the Hamiltonian (11) becomes $H_{\text{eff}} = \Omega_p e^{-i\phi} e^{i4\widetilde{\omega}\overline{n}t}\sigma_{eg}^{+} + \text{h.c.}$, with $\overline{n} = 4|\alpha|^2$. For a sufficient large α, such that $4|\widetilde{\omega}|\overline{n} \gg \Omega_p$ (large detuning), it is easy to see that the qubit's state is not changed by the driving pulse, i.e.,

$$\begin{aligned} |g\rangle|2\alpha\rangle_{1'} &\to |g\rangle|2\alpha\rangle_{1'}, \\ |e\rangle|2\alpha\rangle_{1'} &\to |e\rangle|2\alpha\rangle_{1'}. \end{aligned} \tag{13}$$

After returning to the original interaction picture by performing a unitary operation $U = e^{-iH_0}$, we have from Eqs. (12) and (13)

$$\begin{aligned} |g\rangle|0\rangle_{1'} &\to \left(e^{i\widetilde{\omega}t}\cos\Omega_p t\,|g\rangle - ie^{-i\phi}e^{-i\widetilde{\omega}t}\sin\Omega_p t\,|e\rangle\right)|0\rangle_{1'}, \\ |e\rangle|0\rangle_{1'} &\to \left(-ie^{i\phi}e^{i\widetilde{\omega}t}\sin\Omega_p t\,|g\rangle + e^{-i\widetilde{\omega}t}\cos\Omega_p t\,|e\rangle\right)|0\rangle_{1'}, \end{aligned} \tag{14}$$

and

$$\begin{aligned} |g\rangle|2\alpha\rangle_{1'} &\to e^{i\widetilde{\omega}t}|g\rangle\left|e^{i2\widetilde{\omega}t}2\alpha\right\rangle_{1'}, \\ |e\rangle|2\alpha\rangle_{1'} &\to e^{-i\widetilde{\omega}t}|e\rangle\left|e^{-i2\widetilde{\omega}t}2\alpha\right\rangle_{1'}. \end{aligned} \tag{15}$$

In the next section, we will show how to use the results (3), (8), (14) and (15) to transfer entangled states from n PO qubits to n WO qubits.

3 Transfer of SPS-qubit entangled states onto CS-qubits

The setup is shown in Fig. 1(a). Initially, the coupler qutrit is in the ground state $|g\rangle$ and decoupled from the cavity system. The n SPS qubits are initially in the entangled state

$$c|0\rangle_1|0\rangle_2\cdots|0\rangle_n + d|1\rangle_1|1\rangle_2\cdots|1\rangle_n, \tag{16}$$

where $|0\rangle$ and $|1\rangle$ are the vacuum state and the single-photon state.

Suppose that each of the n cavities $(1', 2', \cdots, n')$ is in a coherent state $|\alpha\rangle$. Thus, the initial state of the whole system is given by

$$\begin{aligned} &\left(c|0\rangle_1|0\rangle_2\cdots|0\rangle_n + d|1\rangle_1|1\rangle_2\cdots|1\rangle_n\right) \\ &|\alpha\rangle_{1'}|\alpha\rangle_{2'}\cdots|\alpha\rangle_{n'}|g\rangle, \end{aligned} \tag{17}$$

where subscripts $1, 2, \cdots, n$ represent cavities $1, 2, \cdots, n$ and subscripts $1', 2', \cdots, n'$ represent cavities $1', 2', \cdots, n'$, respectively. The procedure for transferring the entangled state is listed below:

Step (i): The purpose of this step is to convert the states $|0\rangle$ and $|1\rangle$ of each of cavities $(2, 3, \cdots, n)$ into $|+\rangle$ and $|-\rangle$, respectively. Here, $|\pm\rangle = (|0\rangle \pm |1\rangle)/\sqrt{2}$. Note that this state convertion can be easily implemented by performing local resonant operations on cavity j and an auxilliary qubit j (initially in the ground state) placed in cavity j, i.e., applying resonant interaction of qubit j with cavity j and resonant interaction of qubit j with a classical pulse [32]. After this step of operation, the state (17) becomes

$$\begin{aligned} &\left(c|0\rangle_1|+\rangle_2|+\rangle_3\cdots|+\rangle_n + d|1\rangle_1|-\rangle_2|-\rangle_3\cdots|-\rangle_n\right) \\ &|\alpha\rangle_{1'}|\alpha\rangle_{2'}\cdots|\alpha\rangle_{n'}|g\rangle. \end{aligned} \tag{18}$$

Step (ii): Adjust the level spacings of the coupler qutrit to have cavity 1 on resonance with the $|g\rangle \leftrightarrow |e\rangle$ transition. According to Eq. (3), one has $|0\rangle_1|g\rangle \to |0\rangle_1|g\rangle$ and $|1\rangle_1|g\rangle \to -i|0\rangle_1|e\rangle$ for an interaction time $t = \pi/(2g_r)$. Hence, the state (18) becomes

$$\begin{aligned} &|0\rangle_1\left(c|g\rangle|+\rangle_2|+\rangle_3\cdots|+\rangle_n - id|e\rangle|-\rangle_2|-\rangle_3\cdots|-\rangle_n\right) \\ &|\alpha\rangle_{1'}|\alpha\rangle_{2'}\cdots|\alpha\rangle_{n'}. \end{aligned} \tag{19}$$

Then, the level spacings of the coupler qutrit is adjusted back such that the qutrit is decoupled from cavity 1.

Step (iii): Adjust the level spacings of the coupler qutrit so that the qutrit is off resonant with the cavities $(2, 3, \cdots, n, 1', 2', \cdots, n')$ [Fig. 1(b)] to achieve an effective Hamiltonian (7). According to Eq. (8), the state (19) changes to

$$\begin{aligned} &|0\rangle_1\Big[c|g\rangle\left(|0\rangle_2 + e^{i\lambda_2 t}|1\rangle_2\right)\left(|0\rangle_3 + e^{i\lambda_3 t}|1\rangle_3\right)\cdots \\ &\left(|0\rangle_n + e^{i\lambda_n t}|1\rangle_n\right)|\alpha\rangle_{1'}|\alpha\rangle_{2'}..|\alpha\rangle_{n'} - id|e\rangle|-\rangle_2|-\rangle_3\cdots \\ &|-\rangle_n\left|e^{i\lambda_{1'}t}\alpha\right\rangle_{1'}\left|e^{i\lambda_{2'}t}\alpha\right\rangle_{2'}..\left|e^{i\lambda_{n'}t}\alpha\right\rangle_{n'}\Big]. \end{aligned} \tag{20}$$

Now let us set

$$|\lambda_2| = |\lambda_3|\cdots = |\lambda_n| = \lambda, \quad |\lambda_{1'}| = |\lambda_{2'}|\cdots = |\lambda_{n'}| = \lambda. \tag{21}$$

Thus, for an interaction time $t = \pi/\lambda$, the state (20) becomes

$$|0\rangle_1|-\rangle_2|-\rangle_3\cdots|-\rangle_n\left(c|g\rangle|\alpha\rangle_{1'}|\alpha\rangle_{2'}\cdots|\alpha\rangle_{n'}\right.$$

$$-\mathrm{i}d\left|e\right\rangle\left|-\alpha\right\rangle_{1'}\left|-\alpha\right\rangle_{2'}\cdots\left|-\alpha\right\rangle_{n'}\big). \tag{22}$$

Then, the level spacings of the qutrit is adjusted back such that the qutrit is decoupled from the $2n$ cavities.

Step (iv): Apply a classical driving field on resonance with cavity $1'$ to obtain a displacement operator $D\left(\alpha\right)$ in phase space, which results in the transformation $\left|\alpha\right\rangle_{1'}\rightarrow\left|2\alpha\right\rangle_{1'}$ and $\left|-\alpha\right\rangle_{1'}\rightarrow\left|0\right\rangle_{1'}$. Thus, we have from Eq. (22)

$$\begin{aligned}&\left|0\right\rangle_{1}\left|-\right\rangle_{2}\left|-\right\rangle_{3}\cdots\left|-\right\rangle_{n}\big(c\left|g\right\rangle\left|2\alpha\right\rangle_{1'}\left|\alpha\right\rangle_{2'}..\left|\alpha\right\rangle_{n'}\\&-\mathrm{i}d\left|e\right\rangle\left|0\right\rangle_{1'}\left|-\alpha\right\rangle_{2'}\cdots\left|-\alpha\right\rangle_{n'}\big).\end{aligned} \tag{23}$$

Step (v): Adjust the frequency of cavity $1'$ to have it off resonant with the $\left|g\right\rangle\leftrightarrow\left|e\right\rangle$ transition of the qutrit. Meanwhile apply a classical pulse (with initial phase $\phi=\pi$ and frequency $\omega_p=\omega_{eg}+\widetilde{g}^2/\widetilde{\Delta}$) to the qutrit. According to Eqs. (14) and (15), for $t=\pi/\left(2\Omega_p\right)$, we have $\left|e\right\rangle\left|0\right\rangle_{1'}\rightarrow\mathrm{i}\mathrm{e}^{\mathrm{i}\widetilde{\omega}t}\left|g\right\rangle\left|0\right\rangle_{1'}$ while the state $\left|g\right\rangle\left|2\alpha\right\rangle_{1'}$ becomes $\mathrm{e}^{\mathrm{i}\widetilde{\omega}t}\left|g\right\rangle\left|\mathrm{e}^{\mathrm{i}2\widetilde{\omega}t}2\alpha\right\rangle_{1'}$. Thus, we have from Eq. (23)

$$\begin{aligned}&\mathrm{e}^{\mathrm{i}\widetilde{\omega}t}\left|g\right\rangle\left|0\right\rangle_{1}\left|-\right\rangle_{2}\left|-\right\rangle_{3}\cdots\left|-\right\rangle_{n}\Big\{c\left|\mathrm{e}^{\mathrm{i}2\widetilde{\omega}t}2\alpha\right\rangle_{1'}\left|\alpha\right\rangle_{2'}\cdots\left|\alpha\right\rangle_{n'}\\&+d\left|0\right\rangle_{1'}\left|-\alpha\right\rangle_{2'}\cdots\left|-\alpha\right\rangle_{n'}\Big\}.\end{aligned} \tag{24}$$

If the operation time of this step satisfies $2\widetilde{\omega}t=2m\pi$ (m is an integer), we have $\mathrm{e}^{\mathrm{i}2\widetilde{\omega}t}=1$. Thus, the state (24) becomes

$$\begin{aligned}&\left|g\right\rangle\left|0\right\rangle_{1}\left|-\right\rangle_{2}\left|-\right\rangle_{3}\cdots\left|-\right\rangle_{n}\big(c\left|2\alpha\right\rangle_{1'}\left|\alpha\right\rangle_{2'}\cdots\left|\alpha\right\rangle_{n'}\\&+d\left|0\right\rangle_{1'}\left|-\alpha\right\rangle_{2'}\cdots\left|-\alpha\right\rangle_{n'}\big),\end{aligned} \tag{25}$$

where we have dropped off the global phase $\mathrm{e}^{\mathrm{i}\widetilde{\omega}t}$. After this step of operation, the frequency of cavity $1'$ is adjusted such that cavity $1'$ is decoupled from the qutrit.

Step (vi): Apply a classical driving field on resonance with cavity $1'$, to obtain a displacement operator $D\left(-\alpha\right)$ resulting in the transformation $\left|2\alpha\right\rangle_{1'}\rightarrow\left|\alpha\right\rangle_{1'}$ and $\left|0\right\rangle_{1'}\rightarrow\left|-\alpha\right\rangle_{1'}$. Hence, we have from Eq. (25)

$$\begin{aligned}&\left|g\right\rangle\left|0\right\rangle_{1}\left|-\right\rangle_{2}\left|-\right\rangle_{3}\cdots\left|-\right\rangle_{n}\otimes\big(c\left|\alpha\right\rangle_{1'}\left|\alpha\right\rangle_{2'}\cdots\left|\alpha\right\rangle_{n'}\\&+d\left|-\alpha\right\rangle_{1'}\left|-\alpha\right\rangle_{2'}\cdots\left|-\alpha\right\rangle_{n'}\big),\end{aligned} \tag{26}$$

which shows that the n CS qubits ($1'$, $2'$, $\cdots$, n') are in the entangled state $c\left|\alpha\right\rangle_{1'}\left|\alpha\right\rangle_{2'}\cdots\left|\alpha\right\rangle_{n'}+d\left|-\alpha\right\rangle_{1'}\left|-\alpha\right\rangle_{2'}\cdots\left|-\alpha\right\rangle_{n'}$, i.e., the original entangled state (16) of the n SPS qubits has been transferred onto the n CS qubits after the above operations. Here, note that in Eq. (26), the two logic states of CS qubit j' ($j'=1'$, $2'$, $\cdots$, n') are encoded with two coherent states $\left|\alpha\right\rangle$ and $\left|-\alpha\right\rangle$ of cavity j'.

To ensure that each step described above is performed by unitary operations, the two wave vectors in each bracket of Eqs. (24–26) should be orthogonal. Note that this requirement can be met for a large enough α. The reason for this is as follows. Because of $\left|\left\langle\alpha\right|-\alpha\right\rangle\left|=\right|\left\langle2\alpha\right|0\right\rangle\left|=\mathrm{e}^{-2\left|\alpha\right|^2}\right.\right.$, the two coherent states $\left|\alpha\right\rangle$ and $\left|-\alpha\right\rangle$ or the two states $\left|0\right\rangle$ and $\left|2\alpha\right\rangle$ involved in Eqs. (24-26) can be quasi-orthogonal for a sufficiently large α, as mentioned in the introduction.

Several other points need to be made as follows:

(i) As shown above, there is no need of measurement for the state transfer, i.e., all basic operations are unitary. Thus, by performing reverse unitary operations, the entangled state $c\left|\alpha\right\rangle_{1'}\left|\alpha\right\rangle_{2'}\cdots\left|\alpha\right\rangle_{n'}+d\left|-\alpha\right\rangle_{1'}\left|-\alpha\right\rangle_{2'}\cdots\left|-\alpha\right\rangle_{n'}$ of n CS qubits can be converted back into the entangled state $c\left|0\right\rangle_{1}\left|0\right\rangle_{2}\cdots\left|0\right\rangle_{n}+d\left|1\right\rangle_{1}\left|1\right\rangle_{2}\cdots\left|1\right\rangle_{n}$ of n SPS qubits when the dissipation of the system is negligible.

(ii) The total operation time for the state transfer is

$$t_{\mathrm{op}}=\pi/\lambda+\pi/\left(2g_r\right)+\pi/\left(2\Omega_p\right)+\tau_p+2\tau_\alpha+4\tau_d+2\tau_c, \tag{27}$$

which does not depend on the number of qubits involved in the entangled state. Here, τ_p is the typical time for converting the states $\left|0\right\rangle$ and $\left|1\right\rangle$ of each of cavities (2, 3, $\cdots$, n) into $\left|\pm\right\rangle$, τ_α is the typical time for performing a displacement operation on the cavity's coherent state, τ_d is the typical time required for adjusting the level spacings of the coupler qutrit, and τ_c is the typical time for adjusting the cavity frequency.

(iii) The state transfer requires adjusting the qutrit's level spacings to have the qutrit coupled with (or decoupled from) the cavities. For superconducting devices, their level spacings can be rapidly (within 1–3 ns) adjusted by varying external control parameters [33, 34]. In addition, as shown above, the frequency of cavity $1'$ needs to be adjusted to have cavity $1'$ coupled with (or decoupled from) the qutrit. Note that for superconducting microwave cavities, the cavity frequencies can be fast (within a few nanoseconds) tuned in experiments [35, 36].

(iv) Because of $\lambda_j=g_j^2/\Delta_j$ and $\lambda_{j'}=\mu_{j'}^2/\Delta_{j'}$, the condition (21) turns out into

$$\begin{aligned}\frac{g_2^2}{\left|\Delta_2\right|}=\frac{g_3^2}{\left|\Delta_3\right|}=\cdots=\frac{g_n^2}{\left|\Delta_n\right|}=\frac{\mu_{1'}^2}{\left|\Delta_{1'}\right|}=\frac{\mu_{2'}^2}{\left|\Delta_{2'}\right|}=\frac{\mu_{3'}^2}{\left|\Delta_{3'}\right|}\\=\cdots=\frac{\mu_{n'}^2}{\left|\Delta_{n'}\right|}.\end{aligned} \tag{28}$$

Due to $\Delta_j=\omega_{fg}-\omega_{c_j}$ (2, 3, $\cdots$, n) and $\Delta_{j'}=\omega_{fe}-\omega_{c_{j'}}$ ($1'$, $2'$, $\cdots$, n'), the equality given in Eq. (28) can be easily established by carefully selecting Δ_j (via adjusting the frequency ω_{c_j} of cavity j) and carefully selecting $\Delta_{j'}$ (via adjusting the frequency $\omega_{c_{j'}}$ of cavity j').

(v) As described above, for step (v), the operation time should satify both $t=\pi/\left(2\Omega_p\right)$ and $2\widetilde{\omega}t=2m\pi$, i.e.,

$$\Omega_p=\frac{\widetilde{g}^2}{4m\widetilde{\Delta}}, \tag{29}$$

which can be easily met by adjusting the Rabi frequency of the pulse.

The present proposal works out for either $c=d$ or $c\neq d$. Note that the case of $c=d$ is specially interesting, because

Bell states and GHZs are of great importance in quantum communication and QIP. It should be mentioned that how to directly prepare the initial entangled state (16) with $c = d$ was previously reported [37]. Alternatively, the state (16) with $c = d$ can be created by preparing n natural or artificial atoms (distributed in n cavities) in a maximally entangled state $|g\rangle_1 |g\rangle_2 \cdots |g\rangle_n + |e\rangle_1 |e\rangle_2 \cdots |e\rangle_n$ [38–42] and then having each atom (in the excited state $|e\rangle$) emitting a single photon into its cavity through local operations on each atom and its cavity.

4 Possible experimental implementation

This section is aimed at investigating the experimental feasibility for transferring a Bell state of two SPS qubits $(1, 2)$ onto two CS qubits $(1', 2')$, by considering four 3D microwave cavities coupled to a superconducting flux qutrit [Fig. 2(a)]. In the following, we will briefly discuss the fidelity for the Bell state transfer, which is performed in a more realistic situation. Since steps (i), (ii), (iv) and (vi) employ only the resonant interactions, these steps can be completed within a very short time. In this sense, the influence of the qutrit decoherence, the cavity decay, and the inter-cavity crosstalk is negligibly small for steps (i), (ii), (iv) and (vi). Therefore, the imperformance of the Bell state transfer is mainly caused by the system dissipation and the inter-cavity crosstalk during the operation of steps (iii) and (v), because these steps require reletively long operation times due to the use of the qutrit-cavity off-resonant interaction.

After taking into account the unwanted couplings between the qutrit's level transitions and the cavities as well as the inter-cavity crosstalk, the Hamiltonian H_2 in Eq. (4), with $n = 2$ and $n' = 2'$ for the present case, is modified as

$$\begin{aligned} H_2' = & \left(g_2 e^{i\Delta_2 t}\hat{a}_2\sigma_{fg}^+ + g_2' e^{i\Delta_2' t}\hat{a}_2\sigma_{fe}^+ \right. \\ & \left. + g_2'' e^{i\Delta_2'' t}\hat{a}_2\sigma_{eg}^+ + \text{h.c.}\right) \\ & + \left(\mu_{1'} e^{i\Delta_{1'} t}\hat{b}_{1'}\sigma_{fe}^+ + \mu_{1'}' e^{i\Delta_{1'}' t}\hat{b}_{1'}\sigma_{fg}^+ \right. \\ & \left. + \mu_{1'}'' e^{i\Delta_{1'}'' t}\hat{b}_{1'}\sigma_{eg}^+ + \text{h.c.}\right) \\ & + \left(\mu_{2'} e^{i\Delta_{2'} t}\hat{b}_{2'}\sigma_{fe}^+ + \mu_{2'}' e^{i\Delta_{2'}' t}\hat{b}_{2'}\sigma_{fg}^+ \right. \\ & \left. + \mu_{2'}'' e^{i\Delta_{2'}'' t}\hat{b}_{2'}\sigma_{eg}^+ + \text{h.c.}\right) \\ & + \varepsilon, \end{aligned} \tag{30}$$

where the second (third) term in line one describes the unwanted coupling between cavity 2 and the $|e\rangle \to |f\rangle$ ($|g\rangle \to |e\rangle$) transition with coupling constant g_2' (g_2'') and detuning $\Delta_2' = \omega_{fe} - \omega_{c_2}$ ($\Delta_2'' = \omega_{eg} - \omega_{c_2}$), the second (third) term in line two describes the unwanted coupling between cavity $1'$ and the $|g\rangle \to |f\rangle$ ($|g\rangle \to |e\rangle$) transition with coupling constant $\mu_{1'}'$ ($\mu_{1'}''$) and detuning $\Delta_{1'}' = \omega_{fg} - \omega_{c_{1'}}$ ($\Delta_{1'}'' = \omega_{eg} - \omega_{c_{1'}}$), and the second (third) term in line three describes the unwanted coupling between cavity $2'$ and the $|g\rangle \to |f\rangle$ ($|g\rangle \to |e\rangle$) transition with coupling constant $\mu_{2'}'$ ($\mu_{2'}''$) and detuning $\Delta_{2'}' = \omega_{fg} - \omega_{c_{2'}}$ ($\Delta_{2'}'' = \omega_{eg} - \omega_{c_{2'}}$). In addition, ε is the Hamiltonian describing the inter-cavity crosstalk, which is given by

$$\begin{aligned} \varepsilon = & \left(g_{12} e^{i\Delta_{12} t}\hat{a}_1^+\hat{a}_2 + \text{h.c.}\right) + \left(g_{1'2'} e^{i\Delta_{1'2'} t}\hat{b}_{1'}^+\hat{b}_{2'} + \text{h.c.}\right) \\ & + \left(g_{11'} e^{i\Delta_{11'} t}\hat{a}_1^+\hat{b}_{1'} + \text{h.c.}\right) + \left(g_{12'} e^{i\Delta_{12'} t}\hat{a}_1^+\hat{b}_{2'} + \text{h.c.}\right) \\ & + \left(g_{21'} e^{i\Delta_{21'} t}\hat{a}_2^+\hat{b}_{1'} + \text{h.c.}\right) + \left(g_{22'} e^{i\Delta_{22'} t}\hat{a}_2^+\hat{b}_{2'} + \text{h.c.}\right), \end{aligned} \tag{31}$$

where g_{kl} is the crosstalk strength between the two cavities k and l while $\Delta_{kl} = \omega_{c_k} - \omega_{c_l}$ is the frequency difference of the two cavities k and l ($k, l \in \{1, 2, 1', 2'\}; k \neq l$).

On the other hand, when the unwanted couplings between the qutrit's level transitions and cavity $1'$ are considered, the Hamiltonian H_3 in Eq. (9) is modified as

$$\begin{aligned} H_3' = & \left(\tilde{g} e^{i\tilde{\Delta} t}\hat{a}_{1'}\sigma_{eg}^+ + \tilde{g}' e^{i\tilde{\Delta}' t}\hat{a}_{1'}\sigma_{fg}^+ + \tilde{g}'' e^{i\tilde{\Delta}'' t}\hat{a}_{1'}\sigma_{fe}^+ + \text{h.c.}\right) \\ & + \left(\Omega_p e^{-i[(\omega_p - \omega_{eg})t + \phi]}\sigma_{eg}^+ + \Omega_p' e^{-i[(\omega_p - \omega_{fg})t + \phi]}\sigma_{fg}^+ \right. \\ & \left. + \Omega_p'' e^{-i\left[(\omega_p - \omega_{fe})t + \phi\right]}\sigma_{fe}^+ + \text{h.c.}\right), \end{aligned} \tag{32}$$

where the second (third) term in line one describes the unwanted coupling between cavity $1'$ and the $|g\rangle \to |f\rangle$

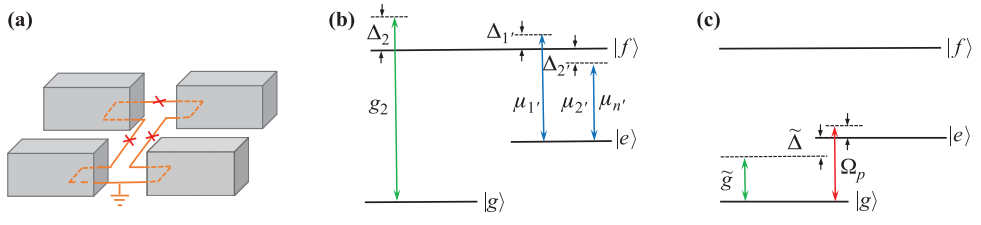

Fig. 2 **(a)** Schematic circuit of four 3D microwave cavities coupled to a superconducting flux qutrit. The qutrit consists of three Josephson junctions and a superconducting loop. **(b)** Illustration of cavity 2 off resonant with the $|g\rangle \leftrightarrow |f\rangle$ transition of the qutrit, while cavities $1'$ and $2'$ off resonant with the $|e\rangle \leftrightarrow |f\rangle$ transition of the qutrit. **(c)** Illustration of cavity $1'$ and a microwave pulse off resonant with the $|g\rangle \leftrightarrow |e\rangle$ transition of the qutrit. The unwanted couplings or interactions of the qutrit's energy-level transitions with the cavities or the pulse are not illustrated in (b) and (c) for simplicity, which however are considered in our numerical simulation, as described in the Hamiltonians (30) and (32).

($|e\rangle \to |f\rangle$) transition with coupling constant $\tilde{g}'$ ($\tilde{g}''$) and detuning $\widetilde{\Delta}' = \omega_{fg} - \widetilde{\omega}_{c_{1'}}$ ($\widetilde{\Delta}'' = \omega_{fe} - \widetilde{\omega}_{c_{1'}}$), while the second (third) term in line two describes the unwanted coupling between the microwave pulse and the $|g\rangle \to |f\rangle$ ($|e\rangle \to |f\rangle$) transition with Rabi frequency Ω_p' (Ω_p''). For simplicity, we here assume that during the operation of step (v), all other cavities are decoupled from the qutrit and the inter-cavity crosstalk is negligible, which can be achieved by adjusting the cavity frequencies such that the cavity-cavity frequency differences are sufficiently large.

During the operation of steps (iii) and (v), the dynamics of the lossy system is determined by

$$\begin{aligned}\frac{\mathrm{d}\rho}{\mathrm{d}t} = & -\mathrm{i}\left[H_{\mathrm{i}}', \rho\right] + \sum_{j=1}^{2} \kappa_j \mathcal{L}\left[\hat{a}_j\right] + \sum_{j'=1'}^{2'} \kappa_{j'} \mathcal{L}\left[\hat{b}_{j'}\right] \\ & + \gamma_{eg} \mathcal{L}\left[\sigma_{eg}^{-}\right] + \gamma_{fe} \mathcal{L}\left[\sigma_{fe}^{-}\right] + \gamma_{fg} \mathcal{L}\left[\sigma_{fg}^{-}\right] \\ & + \gamma_{e,\varphi}\left(\sigma_e \rho \sigma_e - \sigma_e \rho/2 - \rho \sigma_e/2\right) \\ & + \gamma_{f,\varphi}\left(\sigma_f \rho \sigma_f - \sigma_f \rho/2 - \rho \sigma_f/2\right), \end{aligned} \tag{33}$$

where H_{i}' is the modified Hamiltonian H_2' or H_3' given above, $L[\Lambda] = \Lambda\rho\Lambda^{+} - \Lambda^{+}\Lambda\rho/2 - \rho\Lambda^{+}\Lambda/2$ (with $\Lambda = \hat{a}_j, , \hat{b}_{j'}, \sigma_{eg}^{-}, \sigma_{fe}^{-}, \sigma_{fg}^{-}$), $\sigma_{eg}^{-} = |g\rangle\langle e|$, $\sigma_{fe}^{-} = |e\rangle\langle f|$, $\sigma_{fg}^{-} = |g\rangle\langle f|$, $\sigma_e = |e\rangle\langle e|$, and $\sigma_f = |f\rangle\langle f|$. In addition, κ_j ($\kappa_{j'}$) is the decay rate of cavity j (j'); γ_{eg} is the energy relaxation rate for the level $|e\rangle$ of the qutrit corresponding to the decay path $|e\rangle \to |g\rangle$; γ_{fe} (γ_{fg}) is the relaxation rate for the level $|f\rangle$ of the qutrit associated with the decay path $|f\rangle \to |e\rangle$ ($|f\rangle \to |g\rangle$); $\gamma_{e,\varphi}$ ($\gamma_{f,\varphi}$) is the dephasing rate of the level $|e\rangle$ ($|f\rangle$) of the qutrit.

For two SPS qubits, the Bell state is given by Eq. (16) with $c = d = 1/\sqrt{2}$, $n = 2$, i.e., the Bell state is $\frac{1}{\sqrt{2}}\left(|0\rangle_1 |0\rangle_2 + |1\rangle_1 |1\rangle_2\right)$, where the subscripts 1 and 2 represent SPS qubits 1 and 2, respectively. The initial state of the whole system is $\frac{1}{\sqrt{2}}\left(|0\rangle_1 |0\rangle_2 + |1\rangle_1 |1\rangle_2\right)|\alpha\rangle_{1'}|\alpha\rangle_{2'}|g\rangle$, where the subscripts $1'$ and $2'$ represent CS qubits $1'$ and $2'$, respectively. According to Eq. (26), the ideal output state of the whole system after the entire operation is

$$|g\rangle|0\rangle_1|-\rangle_2 \otimes \frac{1}{\sqrt{2}}\left(|\alpha\rangle_{1'}|\alpha\rangle_{2'} + |-\alpha\rangle_{1'}|-\alpha\rangle_{2'}\right). \tag{34}$$

The fidelity of the entire operation is defined as $F = \sqrt{\langle\psi_{id}|\rho|\psi_{id}\rangle}$, where $|\psi_{id}\rangle$ is the ideal output state given by Eq. (34), while ρ is the final density matrix obtained by numerically solving the master equation in a realistic situation.

For a flux qutrit, the typical transition frequency between neighboring levels can be made as 1 to 20 GHz. As an example, consider $\omega_{eg}/(2\pi) = 8.0$ GHz, $\omega_{fe}/(2\pi) = 12.0$ GHz, and $\omega_{fg}/(2\pi) = 20.0$ GHz. Choose $\omega_{c_1}/(2\pi) = 5.0$ GHz for cavity 1. With a choice of $\Delta_2/(2\pi) = -250$ MHz, $\Delta_{1'}/(2\pi) = -125$ MHz, and $\Delta_{2'}/(2\pi) = 125$ MHz, the cavity frequencies are $\omega_{c_2}/(2\pi) = 20.25$ GHz, $\omega_{c_{1'}}/(2\pi) = 12.125$ GHz, and $\omega_{c_{2'}}/(2\pi) = 11.875$ GHz. Thus, we have $\Delta_2'/(2\pi) = -8.25$ GHz, $\Delta_2''/(2\pi) = -12.25$ GHz, $\Delta_{1'}'/(2\pi) = 7.875$ GHz, $\Delta_{1'}''/(2\pi) = -4.125$ GHz, $\Delta_{2'}'/(2\pi) = 8.125$ GHz, and $\Delta_{2'}''/(2\pi) = -3.875$ GHz. For the values of the cavity frequencies here, a simple calculation gives $\Delta_{12}/(2\pi) = -15.25$ GHz, $\Delta_{1'2'}/(2\pi) = 0.25$ GHz, $\Delta_{11'}/(2\pi) = -7.125$ GHz, $\Delta_{12'}/(2\pi) = -6.875$ GHz, $\Delta_{21'}/(2\pi) = 8.125$ GHz, and $\Delta_{22'}/(2\pi) = 8.375$ GHz. In addition, we have $\mu_{1'} = \mu_{2'} = g_2/\sqrt{2}$ according to Eq. (28).

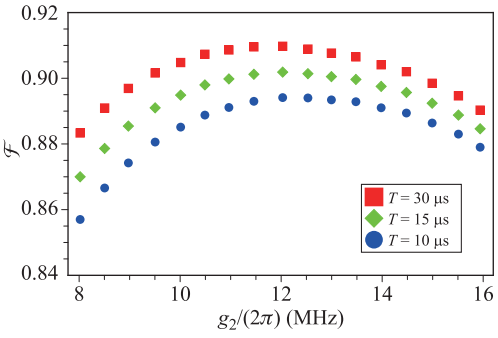

Fig. 3 Fidelity versus g_2. The parameters used in the numerical simulation are referred to the text.

We choose $\widetilde{\Delta}/(2\pi) = 160$ MHz, resulting in $\widetilde{\omega}_{c_{1'}}/(2\pi) = 7.84$ GHz. For the value of $\widetilde{\omega}_{c_{1'}}$ here and the values of ω_{eg}, ω_{fe}, ω_{fg} given above, we have $\widetilde{\Delta}'/(2\pi) = 12.16$ GHz and $\widetilde{\Delta}''/(2\pi) = 4.16$ GHz. We choose $\tilde{g}/(2\pi) = 24.1$ MHz, and thus $\Omega_p/(2\pi) \sim 0.454$ MHz (calculated according to Eq. (29) for $m = 1$ and $\alpha = 1.86$). Because of $\omega_p = \omega_{eg} + \tilde{g}^2/\widetilde{\Delta}$, the driving field frequency ω_p can be calculated given the values of ω_{eg}, $\tilde{g}$, and $\widetilde{\Delta}$ here.

The dipole matrix element χ_{fg} between the two levels $|g\rangle$ and $|f\rangle$, the dipole matrix element χ_{fe} between the two levels $|e\rangle$ and $|f\rangle$, and the dipole matrix element χ_{eg} between the two levels $|g\rangle$ and $|e\rangle$ are assumed to have the relationship of $\chi_{fg} \sim \chi_{fe} \sim 4\chi_{eg}$, which can be made with appropriate design of the qutrit system [43]. Thus, we choose $g_2' \sim g_2$, $g_2'' \sim 0.25 g_2$; $\mu_{1'}' \sim \mu_{1'}$, $\mu_{1'}'' \sim 0.25\mu_{1'}$; $\mu_{2'}' \sim \mu_{2'}$, $\mu_{2'}'' \sim 0.25\mu_{2'}$; $\tilde{g}' \sim 4\tilde{g}$, $\tilde{g}'' \sim 4\tilde{g}$; and $\Omega_p' \sim 4\Omega_p$, $\Omega_p'' \sim 4\Omega_p$.

Other parameters used in the numerical simulation are: (i) $\gamma_{eg}^{-1} = 4T$ μs, $\gamma_{fe}^{-1} = 2T$ μs, $\gamma_{fg}^{-1} = T$ μs, (ii) $\gamma_{\phi e}^{-1} = \gamma_{\phi f}^{-1} = T$ μs, (iii) $\kappa_1, \kappa_2, \kappa_{1'}, \kappa_{2'} = \kappa$, and (iv) $\alpha = 1.86$. In addition, choose $g_{kl} = 0.01 g_m$ [14], with $g_m = \max\{g_2, \mu_{1'}, \mu_{2'}\}$.

By numerically solving the master equation (33), Fig. 3 is plotted, which illustrates the fidelity versus g_2 for $\kappa^{-1} = 100$ μs and $T = 10$ μs, 15 μs, 30 μs. Note that all other coupling constants can be determined for a given g_2, as described above. In Fig. 3, the optimal values of g_2, corresponding to the peaks of three curve lines, are $2\pi \times 12.03$ MHz for $T = 10$ μs, 15 μs and 30 μs. Next, we plot Fig. 4, which shows the fidelity versus κ^{-1} for $g_2 = 2\pi \times 12.03$ MHz and $T = 10$ μs, 15 μs, 30 μs. From Fig. 4, one can see that the fidelity increases with κ^{-1} and

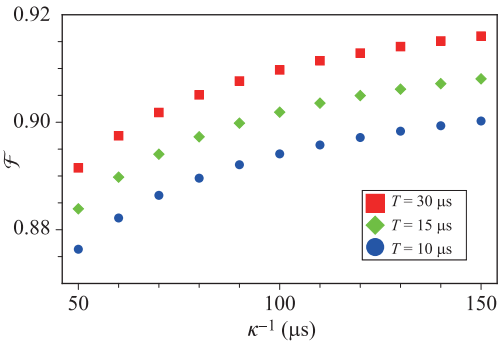

Fig. 4 Fidelity versus κ^{-1}. The parameters used in the numerical simulation are referred to the text.

T, and for $T \geq 15$ μs and $\kappa^{-1} \geq 100$ μs, the fidelity exceeds 90.2%, impling the high-fidelity Bell-state transfer from two SPS qubits onto two CS qubits. It should be mentioned that when taking into account the qutrit decoherence, the cavity decay, and the inter-cavity crosstalk in the operations of steps (i), (ii), (iv) and (vi), the fidelity would be slightly decreased but will not be greatly decreased since these steps of operation can be completed very fast due to the use of the resonant interactions.

The coupling constants are readily achievable because a coupling constant $\sim 2\pi \times 636$ MHz has been reported for a flux device coupled to a microwave cavity [44]. For the parameters chosen above, the state transfer time is estimated as ~ 1.41 μs, which is much shorter than the decoherence times of the coupler qutrit (10–120 μs) and the cavity decay times (50–150 μs) considered in Figs. 3 and 4. For decoherence time of the flux qutrit, a rather conservative case is considered in the numerical simulation, because decoherence time 70 μs to 1 ms for a superconducting flux device has been reported in experiments [45, 46]. For $\kappa^{-1} = 100$ μs and the cavity frequencies $\omega_{c_1}, \omega_{c_2}, \omega_{c_{1'}}, \omega_{c_{2'}}$ given above, a simple calculation gives $Q_1 \sim 3.14 \times 10^6$ for cavity 1, $Q_2 \sim 1.27 \times 10^7$ for cavity 2, $Q_{1'} \sim 7.61 \times 10^6$ for cavity $1'$, and $Q_{2'} \sim 7.46 \times 10^6$ for cavity $2'$. Note that a high quality factor $Q = 3.5 \times 10^7$ of a 3D microwave cavity has been experimentally demonstrated [47]. Our analysis here shows that the high-fidelity transfer of the Bell state of two SPS qubits onto two CS qubits is feasible within the current circuit QED technology.

5 Conclusion

We have explicitally shown how to transfer partially- or maximally-entangled states (including Bell states and GHZ states) of n single-photon-state (SPS) qubits onto n coherent-state (CS) qubits in a circuit-QED system. As shown above, this proposal has these distinguishing features: (i) Only a coupler qutrit is needed, hence the circuit hardware resources is significantly reduced; (ii) The operation time does not increase with the increasing of the number of qubits; (iii) Decoherence from the coupler qutrit is greatly suppressed, because the higher energy level of the coupler qutrit is not excited during the entire operation; and (iv) When the dissipation is negligible, the state transfer is deterministic because of no measurement being performed. Furthermore, we have numerically investigated the experimental feasibility for transferring the Bell state of two SPS qubits onto two CS qubits. The numerical simulation shows that high-fidelity transfer of the Bell state, from two SPS qubits onto two CS qubits, can be achieved with current circuit-QED technology.

Finally, it should be mentioned that since all basic operations are unitary and measurement is not involved, the entangled states of SPS qubits can be transferred back onto CS qubits by performing reverse operations when the dissipation is negligible. This proposal can be applied to transfer maximally- or partially-entangled states between n SPS qubits and n CS qubits in a wide range of physical systems, such as $2n$ microwave or optical cavities coupled to a natural or artificial atom.

Acknowledgements This work was partly supported by the National Natural Science Foundation of China (NSFC) (Grant Nos. 11074062, 11374083, and 11774076), the Key-Area Research and Development Program of GuangDong province (Grant No. 2018B030326001), and the NKRDP of China (Grant No. 2016YFA0301802).

References

1. T. C. Ralph and G. J. Pryde, Optical quantum computation, *Prog. Opt.* 54, 209 (2010)
2. J. L. O'Brien, A. Furusawa, and J. Vučković, Photonic quantum technologies, *Nature Photon.* 3, 687 (2009)
3. Q. Dong, A. J. Torres-Arenas, G. H. Sun, W. C. Qiang, and S. H. Dong, Entanglement measures of a new type pseudo-pure state in accelerated frames, *Front. Phys.* 14(2), 21603 (2019)
4. E. Knill, R. Laflamme, and G. J. Milburn, A scheme for efficient quantum computation with linear optics, *Nature* 409(6816), 46 (2001)
5. P. Zhu, Q. Zheng, S. Xue, C. Wu, X. Yu, Y. Wang, Y. Liu, X. Qiang, J. Wu, and P. Xu, Onchip multiphoton Greenberger–Horne–Zeilinger state based on integrated frequency combs, *Front. Phys.* 15(6), 61501 (2020)
6. H. Jeong and M. S. Kim, Efficient quantum computation using coherent states, *Phys. Rev. A* 65(4), 042305 (2002)
7. M. Mirrahimi, Z. Leghtas, V. V. Albert, S. Touzard, R. J. Schoelkopf, L. Jiang, and M. H. Devoret, Dynamically protected cat-qubits: A new paradigm for universal quantum computation, *New J. Phys.* 16(4), 045014 (2014)
8. J. K. Asbóth, P. Adam, M. Koniorczyk, and J. Janszky, Coherent-state qubits: Entanglement and decoherence, *Eur. Phys. J. D* 30(3), 403 (2004)

9. U. L. Andersen, G. Leuchs, and C. Silberhorn, Continuous-variable quantum information processing, *Laser Photonics Rev.* 4(3), 337 (2010)
10. Z. R. Zhong, J. Q. Sheng, L. H. Lin, and S. B. Zheng, Quantum nonlocality for entanglement of quasiclassical states, *Opt. Lett.* 44(7), 1726 (2019)
11. R. W. Heeres, P. Reinhold, N. Ofek, L. Frunzio, L. Jiang, M. H. Devoret, and R. J. Schoelkopf, Implementing a universal gate set on a logical qubit encoded in an oscillator, *Nat. Commun.* 8(1), 94 (2017)
12. S. E. Nigg, Deterministic Hadamard gate for microwave cat-state qubits in circuit QED, *Phys. Rev. A* 89(2), 022340 (2014)
13. Y. Zhang, X. Zhao, Z. F. Zheng, L. Yu, Q. P. Su, and C. P. Yang, Universal controlled phase gate with cat-state qubits in circuit QED, *Phys. Rev. A* 96(5), 052317 (2017)
14. C. P. Yang and Z. F. Zheng, Deterministic generation of Greenberger–Horne–Zeilinger entangled states of cat-state qubits in circuit QED, *Opt. Lett.* 43(20), 5126 (2018)
15. Y. J. Fan, Z. F. Zheng, Y. Zhang, D. M. Lu, and C. P. Yang, One-step implementation of a multi-target-qubit controlled phase gate with cat-state qubits in circuit QED, *Front. Phys.* 14(2), 21602 (2019)
16. T. Liu, Z. F. Zheng, Y. Zhang, Y. L. Fang, and C. P. Yang, Transferring entangled states of photonic cat-state qubits in circuit QED, *Front. Phys.* 15(2), 21603 (2020)
17. K. Park and H. Jeong, Entangled coherent states versus entangled photon pairs for practical quantum-information processing, *Phys. Rev. A* 82(6), 062325 (2010)
18. P. van Loock, Optical hybrid approaches to quantum information, *Laser Photon. Rev.* 5(2), 167 (2011)
19. S. W. Lee and H. Jeong, Near-deterministic quantum teleportation and resource efficient quantum computation using linear optics and hybrid qubits, *Phys. Rev. A* 87(2), 022326 (2013)
20. C. P. Yang, S. I. Chu, and S. Han, Possible realization of entanglement, logical gates, and quantum information transfer with superconducting-quantum interference-device qubits in cavity QED, *Phys. Rev. A* 67(4), 042311 (2003)
21. J. Q. You and F. Nori, Quantum information processing with superconducting qubits in a microwave field, *Phys. Rev. B* 68(6), 064509 (2003)
22. A. Blais, R. S. Huang, A. Wallraff, S. M. Girvin, and R. J. Schoelkopf, Cavity quantum electrodynamics for superconducting electrical circuits: An architecture for quantum computation, *Phys. Rev. A* 69(6), 062320 (2004)
23. J. Clarke and F. K. Wilhelm, Superconducting quantum bits, *Nature* 453(7198), 1031 (2008)
24. J. Q. You and F. Nori, Atomic physics and quantum optics using superconducting circuits, *Nature* 474(7353), 589 (2011)
25. Z. L. Xiang, S. Ashhab, J. Q. You, and F. Nori, Hybrid quantum circuits: Superconducting circuits interacting with other quantum systems, *Rev. Mod. Phys.* 85(2), 623 (2013)
26. X. Gu, A. F. Kockum, A. Miranowicz, Y. X. Liu, and F. Nori, Microwave photonics with superconducting quantum circuits, *Phys. Rep.* 718–719, 1 (2017)
27. X. T. Mo and Z. Y. Xue, Single-step multipartite entangled states generation from coupled circuit cavities, *Front. Phys.* 14(3), 31602 (2019)
28. J. Joo, C. W. Lee, S. Kono, and J. Kim, Logical measurement-based quantum computation in circuit-QED, *Sci. Rep.* 9(1), 16592 (2019)
29. A. F. Kockum, A. Miranowicz, S. De Liberato, S. Savasta, and F. Nori, Ultrastrong coupling between light and matter, *Nature Rev. Phys.* 1(1), 19 (2019)
30. S. B. Zheng and G. C. Guo, Efficient scheme for two-atom entanglement and quantum information processing in cavity QED, *Phys. Rev. Lett.* 85(11), 2392 (2000)
31. D. F. V. James, and J. Jerke, Effective Hamiltonian theory and its applications in quantum information, *Can. J. Phys.* 85(6), 625 (2007)
32. C. P. Yang and S. Han, *n*-qubit-controlled phase gate with superconducting quantum interference devices coupled to a resonator, *Phys. Rev. A* 72(3), 032311 (2005)
33. P. J. Leek, S. Filipp, P. Maurer, M. Baur, R. Bianchetti, J. M. Fink, M. Goppl, L. Steffen, and A. Wallraff, Using sideband transitions for two-qubit operations in superconducting circuits, *Phys. Rev. B* 79(18), 180511 (2009)
34. M. Neeley, M. Ansmann, R. C. Bialczak, M. Hofheinz, N. Katz, E. Lucero, A. O'Connell, H. Wang, A. N. Cleland, and J. M. Martinis, Process tomography of quantum memory in a Josephson-phase qubit coupled to a two-level state, *Nat. Phys.* 4(7), 523 (2008)
35. M. Sandberg, C. M. Wilson, F. Persson, T. Bauch, G. Johansson, V. Shumeiko, T. Duty, and P. Delsing, Tuning the field in a microwave resonator faster than the photon lifetime, *Appl. Phys. Lett.* 92(20), 203501 (2008)
36. Z. L. Wang, Y. P. Zhong, L. J. He, H. Wang, J. M. Martinis, A. N. Cleland, and Q. W. Xie, Quantum state characterization of a fast tunable superconducting resonator, *Appl. Phys. Lett.* 102(16), 163503 (2013)
37. C. P. Yang, Q. P. Su, and S. Han, Generation of Greenberger–Horne–Zeilinger entangled states of photons in multiple cavities via a superconducting qutrit or an atom through resonant interaction, *Phys. Rev. A* 86(2), 022329 (2012)
38. C. P. Yang, Q. P. Su, S. B. Zheng, and F. Nori, Entangling superconducting qubits in a multi-cavity system, *New J. Phys.* 18(1), 013025 (2016)
39. W. J. Shan, Y. Xia, Y. H. Chen, and J. Song, Fast generation of *N*-atom Greenberger–Horne–Zeilinger state in separate coupled cavities via transitionless quantum driving, *Quantum Inform. Process.* 15(6), 2359 (2016)
40. J. Heo, M. S. Kang, C. H. Hong, H. Yang, and S. G. Choi, Schemes generating entangled states and entanglement swapping between photons and three-level atoms inside optical cavities for quantum communication, *Quantum Inform. Process.* 16(1), 24 (2017)
41. A. Zheng and J. Liu, Generation of an *N*-qubit Greenberger–Horne–Zeilinger state with distant atoms in bimodal cavities, *J. Phys. B* 44(16), 165501 (2011)

42. P. Xu, D. Wang, L. Ye, and Y. Yu, Preparation and transmission of diversified multi-particle entanglements with spatially separate cavities, *Eur. Phys. J. D* 69(6), 144 (2015)

43. Y. X. Liu, J. Q. You, L. F. Wei, C. P. Sun, and F. Nori, Optical selection rules and phase dependent adiabatic state control in a superconducting quantum circuit, *Phys. Rev. Lett.* 95(8), 087001 (2005)

44. T. Niemczyk, F. Deppe, H. Huebl, E. P. Menzel, F. Hocke, M. J. Schwarz, J. J. Garcia Ripoll, D. Zueco, T. Hümmer, E. Solano, A. Marx, and R. Gross, Circuit quantum electrodynamics in the ultrastrong-coupling regime, *Nat. Phys.* 6(10), 772 (2010)

45. F. Yan, S. Gustavsson, A. Kamal, J. Birenbaum, A. P. Sears, D. Hover, T. J. Gudmundsen, D. Rosenberg, G. Samach, S. Weber, J. L. Yoder, T. P. Orlando, J. Clarke, A. J. Kerman, and W. D. Oliver, The flux qubit revisited to enhance coherence and reproducibility, *Nat. Commun.* 7(1), 12964 (2016)

46. J. Q. You, X. Hu, S. Ashhab, and F. Nori, Low-decoherence flux qubit, *Phys. Rev. B* 75(14), 140515 (2007)

47. M. Reagor, W. Pfaff, C. Axline, R. W. Heeres, N. Ofek, K. Sliwa, E. Holland, C. Wang, J. Blumoff, K. Chou, M. J. Hatridge, L. Frunzio, M. H. Devoret, L. Jiang, and R. J. Schoelkopf, A quantum memory with near-millisecond coherence in circuit QED, *Phys. Rev. B* 94(1), 014506 (2016)